

Article

# Zero Stress Aging of Glass and Carbon Fibers in Water and Oil—Strength Reduction Explained by Dissolution Kinetics

Andreas T. Echtermeyer <sup>1,\*</sup>, Andrey E. Krauklis <sup>1,2,†</sup> , Abedin I. Gagani <sup>1,3</sup> and Erik Sæter <sup>1</sup>

<sup>1</sup> Department of Mechanical and Industrial Engineering, Norwegian University of Science and Technology, 7491 Trondheim, Norway; andykrauklis@gmail.com (A.E.K.); abedin.gagani@tuhh.de (A.I.G.); erik.sater@ntnu.no (E.S.)

<sup>2</sup> SINTEF Industry, Department Materials and Nanotechnology, 0314 Oslo, Norway

<sup>3</sup> Institute of Polymer Composites, Hamburg University of Technology (TUHH), D-21073 Hamburg, Germany

\* Correspondence: andreas.echtermeyer@ntnu.no

† Authors had a similar degree of contribution (see contribution).

Received: 17 October 2019; Accepted: 4 December 2019; Published: 6 December 2019



**Abstract:** Understanding the strength degradation of glass and carbon fibers due to exposure to liquids over time is important for structural applications. A model has been developed for glass fibers that links the strength reduction in water to the increase of the Griffith flaw size of the fibers. The speed of the increase is determined by regular chemical dissolution kinetics of glass in water. Crack growth and strength reduction can be predicted for several water temperatures and pH, based on the corresponding dissolution constants. Agreement with experimental results for the case of water at 60 °C with a pH of 5.8 is reasonably good. Carbon fibers in water and toluene and glass fibers in toluene do not chemically react with the liquid. Subsequently no strength degradation is expected and will be confirmed experimentally. All fiber strength measurements are carried out on bundles. The glass fibers are R-glass.

**Keywords:** glass fibers; carbon fibers; zero stress; environmental; aging; model; dissolution; kinetics; water; oil; strength

## 1. Introduction

The fiber dominated tensile strength of a composite material is an important design parameter. It is typically measured on unidirectional laminates [1,2] or it can be back calculated from cross-plyed or other laminate configurations. Back calculation first requires calculation of the UD elastic constants from the laminate performance [3]. Subsequently, a failure criterion needs to be applied [4,5]. A simple approach to obtain the strength assumes the strain to failure of the fibers does not change, combined with the maximum strain criterion. The data is typically well known for the common fiber-matrix combinations. When using composites in harsh environments over long periods, the fiber dominated strength may drop. The strength reduction with time under such conditions is not well documented and the mechanisms are not completely understood. This lack of understanding is a problem where composites are used with long term exposure to a combination of high temperatures, water and/or oil. Obtaining these data requires extensive test programs that are time consuming and costly.

Using a multiscale approach can potentially simplify the test effort by investigating the performance of the fibers and matrix separately and then predicting many properties of the composite laminate from the constituent's behavior. This paper focuses on one such aspect, the change in strength of the fibers when exposed to water or oil, thereby providing a building block for a full multiscale analysis. (For a full design the complete set of properties is needed.) Glass and carbon fibers exposed to water

and toluene at 60 °C are investigated. Toluene is chosen as a low molecular weight component of oil. The effect of sizing on the fibers also will be analyzed as an important part to understanding the degradation of strength.

The strength reduction with time will be investigated for the simple case where the fibers are exposed to the environment without being loaded, so called “zero stress aging”. Extension of the results to other loading conditions, and to applying the results for composite laminates, will be discussed.

Carbon fibers are typically seen to be chemically inert and should not degrade from exposure to water or toluene. Somewhat surprisingly there seemed to be no documentation of this inertness in the open literature. Glass fibers are known to lose strength with time, as will be described in the next section.

## 2. Modeling Strength Loss of Glass Fibers Due to the Environment

Glass fibers can be seen as a brittle material and the strength of the fiber  $\hat{\sigma}_f$  can be described by the well-known Griffith equation (Equation (1a)) [6] or an equivalent fracture mechanics approach (Equation (1b)):

$$\hat{\sigma}_f = \sqrt{\frac{2E\gamma}{\pi a}} \quad (1a)$$

$$\hat{\sigma}_f = \frac{K_{Ic}}{Y\sqrt{\pi a}} \quad (1b)$$

where  $E$  is the Young’s modulus,  $\gamma$  is the surface energy of the fiber,  $K_{Ic}$  is the fracture toughness and  $a$  is the crack length.  $Y$  is a geometry correction factor for specimens of finite size—values for a rod with a crack can be found in [7].  $Y$  is taken to be constant for the small changes in crack length relevant for this study. A delayed fracture due to environmental attack on the fiber already was attributed to a growth of the flaw by Inglis [8], Griffith [6] and Orowan [9] and further discussed by Charles [10,11]. It was pointed out that the sharpness of the crack must remain constant and blunting of the crack tip would increase the fiber’s strength. This assumption also is used here. It also was postulated that the crack growth velocity should be related to a corrosion rate. Delayed failure due to crack growth would only happen if the corrosion rate of the crack is faster than the corrosion rate of the fiber. When the corrosion rate of the fiber was the same as the crack growth rate, the crack length would not increase because the radius of the fiber would decrease by the same amount as the length of the crack tip grows.

Mathematically the crack length  $a(t)$  can be expressed as:

$$a(t) = a_0 + \left( \frac{da}{dt} - \frac{dr}{dt} \right) t \quad (2)$$

where  $a_0$  is the initial crack length,  $\frac{da}{dt}$  is the crack growth rate or velocity and  $\frac{dr}{dt}$  is the rate of the fiber’s radius change with time.

The growth velocity of a crack in glass was quite extensively studied. The velocity goes through three phases [12]. The initial phase is dependent on the stress intensity factor, the second phase is independent of the stress intensity factor and the final phase is very rapid. Regarding cracks filled with water, the initial phase dominates the crack velocity. It was stated by Freiman, Wiederhorn and Mecholsky [13], that the crack velocity is described by:

$$v = v_0 a_{H_2O} \exp(\Delta G^* / RT) \quad (3)$$

where  $v_0$  is a constant,  $a_{H_2O}$  is the chemical activity of water at the crack tip and  $\Delta G^*$  is the activation free energy of the reaction of at the crack tip.  $R$  and  $T$  are the gas constant and absolute temperature,

respectively. According to Stephen W. Freiman, Sheldon M. Wiederhorn and John J. Mecholsky, Jr. [13]  $\Delta G^*$  is given by:

$$\Delta G^* = -T\Delta S^* + \Delta E^* + P\Delta V^* - \frac{(\gamma^*V^* - \gamma V)}{r_{surface}} \tag{4}$$

where  $r_{surface}$  is the radius of the crack tip,  $\gamma$  is the surface tension of the glass,  $\gamma^*$  is the surface tension of the glass in the activated state,  $V$  is the molar volume of the glass, and  $V^*$  is the molar volume of the glass in the activated state.  $T$  is the absolute temperature,  $\Delta S^*$  the activation entropy,  $\Delta E^*$  the activation energy and  $\Delta V^*$  the activation volume.  $P$  is the pressure at the crack tip, which also depends on the stress intensity factor. Since zero stress experiments were done in this study  $P = 0$ .

The authors of this paper studied the dissolution of glass fibers in distilled water (large “infinite” amount) for sized and unsized fibers. Regarding both cases, the dissolution could be well described with zero-order kinetics [14–16].

$$\frac{\partial m_{fiber}}{\partial t} = -K_0 \xi_{sizing} S(t) \tag{5}$$

Concerning unsized fibers  $\xi_{sizing} = 1$ , for sized fibers the dissolution rate is lower with  $\xi_{sizing} < 1$ . Note that the dissolution rate  $K_0$  needs to be separated in a primary and secondary dissolution rate. This aspect will be added when the experimental results are discussed.

When modeling the glass fiber as a cylinder, mass loss is related to a surface area reduction. The change of mass from Equation (5) can be converted into a change of radius of the fibers with time [16]:

$$r(t) = r_0 - \frac{K_0 \xi_{sizing}}{\rho_{glass}} t \tag{6}$$

The factor  $\frac{K_0 \xi_{sizing}}{\rho_{glass}}$  describes the speed of the dissolution for the glass fibers. As described in Equations (3) and (4), more generally the dissolution speed is dependent on the radius of the surface. To account for the radius dependency the velocity of the dissolution can be given by:

$$v = \vartheta \frac{K_0 \xi_{sizing}}{\rho_{glass}} \tag{7}$$

where  $\vartheta$  is the crack sharpness amplification factor due to the thermodynamics described in Equations (3) and (4), in particular the last term in Equation (4). The factor is a function of the radius of the surface:  $\vartheta \sim \exp\left(-\frac{\gamma^*V^* - \gamma V}{r_{surface}}\right)$ . The dissolution constant  $K_0$  addresses the energy and entropy terms in Equation (4).  $P = 0$  since zero stress aging is investigated here.

When the cracks in the fiber are penetrated by water, the mass loss inside the crack should also be described by Equation (7). Since the radius of the glass fiber and of the crack tip of the flaw in the fiber are very different, the factor  $\vartheta$  is important. The length extension of the crack can then be described by a simple surface mass loss as

$$\Delta a(t) = \vartheta \frac{K_0}{\rho_{glass}} t \tag{8}$$

It is assumed here that the crack tip is not covered by the sizing, i.e.,  $\xi_{sizing} = 1$  for the crack. Equation (8) is valid for any crack geometry, provided there is no preferred dissolution direction in the material, i.e.,  $dr/dt = 0$  in Equation (2). Equations (8) and (9) are based on an implicit assumption that the crack tip radius is constant, i.e.,  $dr/dt = 0$  in Equation (2) during dissolution.

The crack length is then the initial crack length and the crack velocity times time. The crack velocity is given by the difference in crack growth and radius shrinkage of the fiber due to dissolution of the glass in water:

$$a(t) = a_0 + \frac{(\vartheta - \xi_{sizing})K_0}{\rho_{glass}} t \tag{9}$$

Putting the time dependent crack length into the Griffith or fracture toughness equation should allow prediction of strength with time.

$$\hat{\sigma}_f = \sqrt{\frac{2E\gamma}{\pi \left[ a_0 + \frac{(\vartheta - \xi_{sizing}) K_0}{\rho_{glass}} t \right]}} \quad (10a)$$

$$\hat{\sigma}_f = \frac{K_{Ic}}{Y \sqrt{\pi \left[ a_0 + \frac{(\vartheta - \xi_{sizing}) K_0}{\rho_{glass}} t \right]}} \quad (10b)$$

The time dependent strength also can be expressed in relation to the static (short term at  $t = 0$ ) strength  $\hat{\sigma}_{f0}$  giving the same equation for the Griffith or fracture mechanics approach:

$$\hat{\sigma}_f(t) = \frac{\hat{\sigma}_{f0}}{\sqrt{1 + \vartheta \frac{K_0 (\vartheta - \xi_{sizing})}{a_0 \rho_{glass}} t}} \quad (11)$$

Other authors found a similar time dependency of the effect of zero stress aging, but without linking the results directly to dissolution kinetics and using the empirical parameters  $\beta$  and  $\tau$  to modify the Griffith equation:

$$\hat{\sigma}_f(t) = \frac{\hat{\sigma}_{f0}}{\left(1 + \frac{t}{\tau}\right)^\beta} \quad (12)$$

The same time dependency as in Equation (8) ( $\beta = 0.5$ ) was predicted by Schultheisz et. al. [17], based on the predictions by Charles [11]. Experimental data showed that behavior at different temperatures, even though agreement with the formula was not perfect. Similar experimental trends were observed for optical glass fibers [18,19].

Hasløv et al. [20] found a good fit of the data for  $\beta = 0.33$ . Using linear elastic fracture mechanics rather than the Griffith equation, the same empirical relationship as in Equation (12) was obtained [21,22].

### 3. Materials and Methods

#### 3.1. Fiber Bundles

Glass fiber and carbon fiber bundles were tested experimentally.

The glass fibers were boron-free and fluorine-free high strength, high modulus 3B HiPer-Tex™ W2020 R-glass fiber bundles. The average fiber diameter was  $17 \pm 2 \mu\text{m}$  [16,23]. The density of glass ( $\rho_f$ ) was  $2.54 \text{ g/cm}^3$  [16,23]. The authors estimated that a bundle had about 4098 fibers [16]. The Young's modulus of the glass was 86 GPa [23]. The fibers were sized with an epoxy compatible sizing.

Bare glass fibers were obtained by desizing the glass fibers via heat cleaning. The heat cleaning was done at  $565 \text{ }^\circ\text{C}$  for 5 h. It should be noted that the heat cleaning might have had an effect on the density and the chemical nature of the surface layer of glass fibers, which could affect the initial dissolution of the desized glass fibers.

Carbon fibers SOFICAR TORAYCA T700SC 12000-50C (TORAYCA, Tacoma, WA, USA) were used. The bundles were in the shape of a tape, held together by some sort of binder. This binder was immediately soluble in both water and toluene.

#### 3.2. Conditioning of Fiber Bundles

The fiber bundles were conditioned either in a water bath or in a toluene bath under no mechanical loads.

The water bath was filled with distilled water (0.5–1.0 M $\Omega$ -cm) produced via water purification system Aquatron A4000 (Cole–Parmer, Vernon Hills, IL, USA). The pH of the distilled water was  $5.650 \pm 0.010$ , being lower than neutral due to dissolved CO<sub>2</sub> from the atmosphere in equilibrium. The toluene bath was used to represent an oil chemical. Toluene was of environmental grade (99.8+%) obtained from Alfa Aesar (Ward Hill, MA, USA).

The conditioning temperatures of 23 and 60 °C for toluene and water, respectively, was controlled to an accuracy of  $\pm 1$  °C by a PID controller. After, conditioning samples were removed from the bath after 10 min, 5 days, 15 days, 30 days and 90 days for tensile tests. The fibers were dried and stored in air at room temperature before testing. Five to nine fiber bundles were tested per condition. All fiber bundles were tested approximately at the same time after the 90-day conditioning was finished.

### 3.3. Fiber Bundle Tensile Tests

Tensile tests were conducted in air using a servo hydraulic test machine MTS Criterion Model 42 (MTS Systems Corporation, Eden Prairie, MN, USA) with custom grips made for the fiber bundles (seen in Figure 1). The displacement rate was set to 1 mm/min. The temperature during the tests was about 23 °C (room temperature). Tensile tests were performed with 5 specimens for dry samples and for each aging time. The testing rig is shown in Figure 1.



**Figure 1.** Tensile tests of R-glass fiber bundles: (left) the test is running; (right) the glass fiber bundle has failed.

Failure of the glass fiber bundle was detected by a severe drop in the testing load. The maximum load from the load displacement curve was taken as the failure load. The fiber bundle's failure is shown in the right picture of Figure 1—when the fiber bundle fails, it looks as puffy as cotton (there are only a few fibers which are intact), but a few fibers still run from grip to grip. The length of the fiber bundles subjected to tension during tests (i.e., “gauge length”) was 200 mm.

Carbon fiber bundles were tested the same way and showed similar failure behavior.

### 3.4. Fiber Strength and Bundle Strength

Glass and carbon fibers show statistical variation of their strength. Weibull statistics are most widely used to characterize the strength of individual fibers [24]. Getting meaningful statistical data

requires testing of 40–100 individual fibers for one test condition [25]. A simpler way to measure the strength is to test a whole bundle of fibers, especially for comparing different fibers, fiber treatments etc. [26–29]. Assuming the load displacement curves are measured carefully, it also is possible to back calculate the Weibull parameters of individual fibers. This work focused on investigating the relative change of the strength of the fibers after different exposure times to water at 60 °C. Assuming that Weibull and Young’s moduli remain constant, and that exposure to water only changes the characteristic strength of the fibers [22], measuring the peak load of a bundle test is sufficient for exploring the strength changes. The fiber’s peak strength was calculated as the maximum load measured on the bundle divided by the total cross-sectional area of all fibers in a bundle.

The raw data of the tensile load displacement curves for sized R-glass fiber bundles after different conditioning times are shown in Figure 2, as an example. The bundles usually slipped a bit in the grips when loaded, so the displacement is not reflecting the bundle’s behavior. However, not much attention was paid to this effect since the only property of interest was the maximum load from which the fiber strength was calculated. The maximum load could be easily identified.

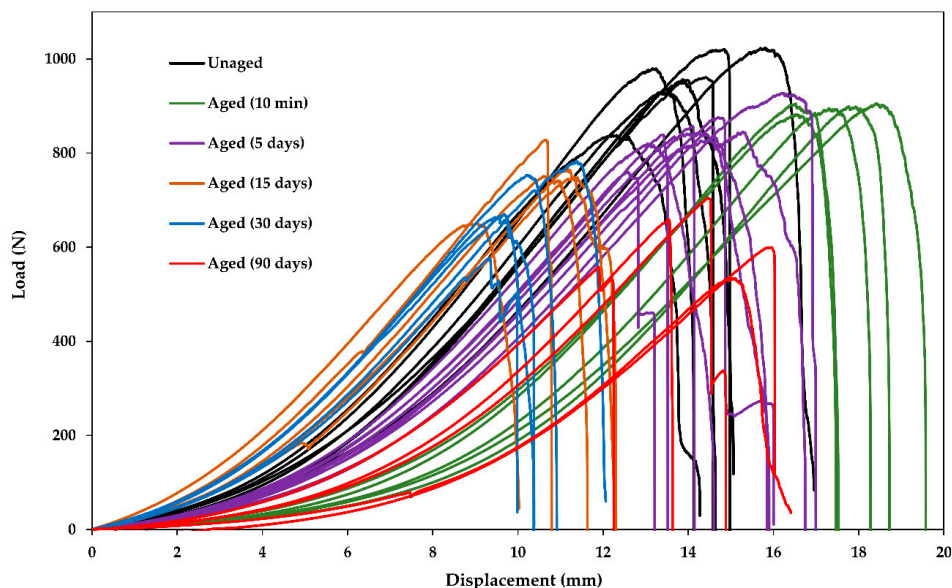


**Figure 2.** Raw data from tensile tests of sized bundles after conditioning (aging) in water up to 90 days.

It should be noted that the initial strength of the fibers, according to the manufacturer datasheets [23,30], are: GF 2700–2900 MPa and CF 4900 MPa. The bundle testing method reported here appears to be underestimating the initial fiber strength by a factor of more than 2. It is likely that such disparity is due to fiber–fiber friction within bundles and/or due to misalignment, which are common issues with fiber bundle strength testing. Since this paper is mainly interested in the relative change of the strength, the low absolute values were not seen as being critical for the results.

## 4. Results

### 4.1. Experimentally Measured Strengths

The test results for bundles from carbon and glass fibers in water and toluene are summarized in Table 1. The complete set of measurements is given in Appendix A.

The strength of desized fibers is very low compared to the sized fibers. There is a significant fundamental strength loss in desized glass fibers from exposure to high temperatures, but the drop measured here is higher than expected. Burning off the sizing and subsequent handling probably severely damages the fibers further, causing this large drop in strength.

**Table 1.** Experimentally obtained tensile bundle strength of aged glass and carbon fiber bundles. Mean  $\pm$  one standard deviation is given.

Aging Time [h]	Sized GF Strength in Water [MPa]	Desized GF Strength in Water [MPa]	Sized GF Strength in Toluene [MPa]	CF Strength in Water [MPa]	CF Strength in Toluene [MPa]
0 (unaged)	1030 $\pm$ 68	185	1030 $\pm$ 68	2086 $\pm$ 111	2086 $\pm$ 111
0.17 (10 min)	986 $\pm$ 10	139	1029 $\pm$ 70	2348 $\pm$ 132	2220 $\pm$ 163
24 (1 day)	-	146	-	-	-
72 (3 days)	-	177	-	-	-
120 (5 days)	910 $\pm$ 48	145	932 $\pm$ 69	2275 $\pm$ 106	2102 $\pm$ 123
192 (8 days)	-	176	-	-	-
240 (10 days)	-	211	-	-	-
360 (15 days)	805 $\pm$ 68	143	928 $\pm$ 14	2295 $\pm$ 122	2217 $\pm$ 114
528 (22 days)	-	205	-	-	-
720 (30 days)	741 $\pm$ 88	220	956 $\pm$ 51	2321 $\pm$ 39	2285 $\pm$ 84
2160 (90 days)	685 $\pm$ 76	-	950 $\pm$ 81	2331 $\pm$ 112	-

#### 4.2. Strength Changes when Fibers Do Not Interact Chemically with the Environment

As expected, data from carbon fibers show basically no change in strength for both aging in water and toluene because carbon fibers are seen to be inert to both liquids. Nonetheless, there is an initial 10% increase in strength. The cause of this increase is not clear. Most likely it is an effect of the test setup. Possibly the fibers in the bundle were not evenly tensioned in the tape and the load was better shared when the binder was dissolved. A similar result was obtained for the sized glass fibers in toluene. It was expected that the glass would not react with the toluene and the strength should not change with time. This was confirmed, but also here, an initial change in strength after short exposures was observed—a drop in strength of roughly 10%. The results are summarized in Figure 3. Within a variation of 10% of the static strength remains constant for carbon fibers aged in glass and water and glass fibers exposed to toluene, i.e., the strength remains approximately constant with time when the fibers do not chemically interact with the environment. A consistent 10% decrease in GF strength was measured for all aged sized GF samples. It may be that it is somehow related to simple geometry, which could affect the fiber–fiber friction within bundles. The CF tow, which is geometrically quite similar, did not demonstrate any strength decrease in toluene. Perhaps some sensitivity of the fiber sizing to this solvent could be a reason for this different response.

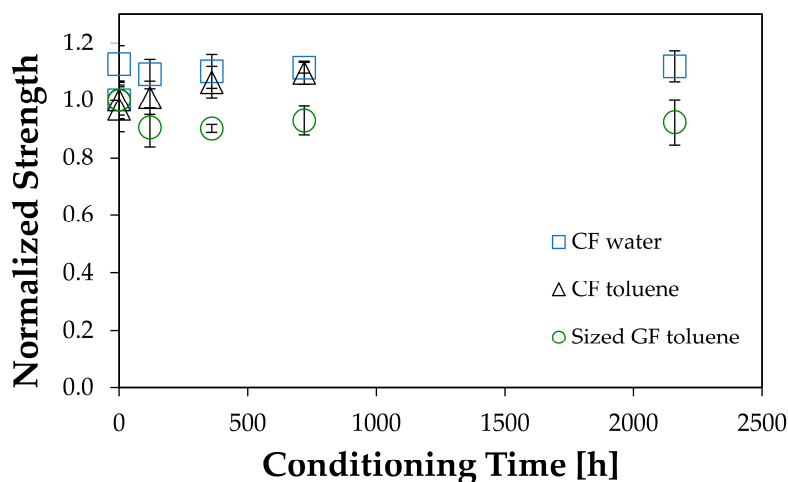


**Figure 3.** Strength change relative to the dry properties due to zeros stress water-induced and toluene-induced aging for bundles of Carbon Fibers CF and Glass Fibers GF. The values on the Y-axis are normalized by the bundle strength of unaged GF and CF.

### 4.3. Strength Changes of Glass Fiber Bundles Interacting Chemically with Water

Sized fiber bundles exposed to water show a clear drop in strength of over 30%, as shown in Figure 4. This drop is larger than the possible experimental error of about 10% observed for fiber bundles exposed to non-interacting liquids as described above. The desized fibers show an about constant strength with time, but the initial strength is unusually low, as discussed above, putting some doubt on the relevance of the results of the desized fibers.

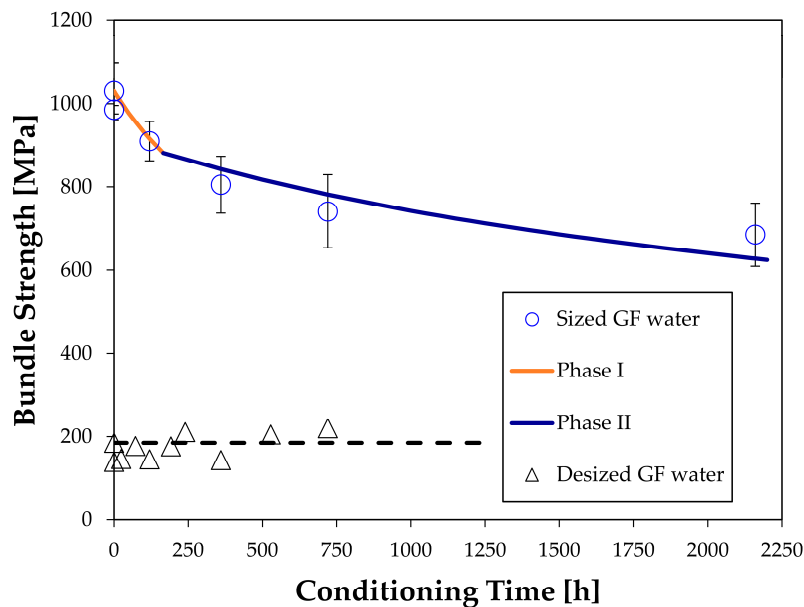


**Figure 4.** Fiber Bundle Strength change due to zero stress aging in water for sized and desized Glass Fibers GF.

Based on the Griffith or fracture mechanics Equation (1a,b) the length  $a_0$  of the initial cracks in the glass fibers can be estimated from the dry strength measurements reported in Table 1:

$$a_0 = \frac{2E\gamma}{\pi \hat{\sigma}_f^2} \text{ or } a_0 = \frac{K_{Ic}^2}{\pi Y^2 \hat{\sigma}_f^2} \quad (13)$$

The surface energy for fracture  $\gamma$  for the R-glass fibers tested here, or even fibers in general, does not seem to be reported in the open literature, except for glass plates, the fracture surface energy was reported for dry flaws to be in the range of 2–5.3 J/m<sup>2</sup> for several types of glasses [31–33]. Since the energy changes not only with glass composition, but also with the temperature and loading rate, the reported values spread quite a bit. Note that the fracture surface energies are not the same as the typically measured surface energies describing wetting, which are about a factor 10 lower [32]. Alternatively, the flaw size can be calculated from the fracture toughness  $K_{Ic}$  of the glass. The value is about 0.7 to 0.8 MPa m<sup>1/2</sup> [31,34]. Additionally, no values could be found in the literature for the R-glass fibers investigated here. The stress amplification factor is taken as  $Y = 1$ , because the cracks are very small compared to the radius of the fibers.

Choosing an average surface energy of 3.7 J/m based on literature data and a Young's modulus  $E$  of 86 GPa [23] the initial crack lengths can be calculated using the dry strength data reported in Table 1.

- sized fibers:  $a_0 = 0.2 \mu\text{m}$
- desized fibers:  $a_0 = 5.9 \mu\text{m}$

Based on Equation (11), it should now be possible to model the strength loss with time if the dissolution constant  $K$  is known, combined with a single crack sharpness amplification factor  $\vartheta$ .

Analyzing the dissolution of glass fibers in a different study [16], the authors found an unsteady-state dissolution (Phase I) occurring up to  $t_{st} = 166$  h with a kinetic constant of  $K_0^I$ . Afterwards, a steady state (Phase II) with a kinetic constant of  $K_0^{II}$  was observed. The dissolution rate of sized fibers was by factor  $\xi_{sizing} = 0.165$  s lower compared to desized fibers [14,15]. The results are summarized in Table 2.

**Table 2.** Dissolution constants for R-glass fiber bundles at 60 °C, after [15,16].

$K_0^I$ (g/m <sup>2</sup> ·s)	$K_0^{II}$ (g/m <sup>2</sup> ·s)	$t_{st}$ (h)	$\xi_{sizing}$
$(1.82 \pm 0.29) \cdot 10^{-8}$	$(4.05 \pm 0.29) \cdot 10^{-9}$	166	0.165

Modifying Equation (11) for two dissolution constants, the strength loss with conditioning time is obtained:

$$\hat{\sigma}_f(t) = \frac{\hat{\sigma}_{f0}}{\sqrt{1 + \frac{K_0^I(\vartheta - \xi_{sizing})}{a_0 \rho_{glass}} t}} \text{ for } t \leq t_{st} \tag{14a}$$

$$\hat{\sigma}_f(t) = \frac{\hat{\sigma}_f^I}{\sqrt{1 + \frac{K_0^{II}(\vartheta - \xi_{sizing})}{a_0 \rho_{glass}} t}} \text{ for } t > t_{st} \tag{14b}$$

and

$$\hat{\sigma}_f^I = \frac{\hat{\sigma}_{f0}}{\sqrt{1 + \frac{K_0^I(\vartheta - \xi_{sizing})}{a_0 \rho_{glass}} t_{st}}} \tag{14c}$$

The experimental and the theoretically predicted curves of the R-glass fiber bundle strength deterioration due to aging are shown in Figure 4. The best least square fit was obtained for  $\vartheta = 993$ . The theoretical curve represents the strength loss of the sized fiber bundles reasonably well. Using the same constants for the unsized bundles, a basically constant strength is predicted, as observed. The reason is that the crack growth velocity is small compared to the initial crack length for the weak desized fibers. The key modeling parameters are listed in Table 3. Note that  $\xi_{sizing}$  is a number between 0 and 1 and is not important here, because  $\vartheta \gg \xi_{sizing}$ .

**Table 3.** Model parameters describing crack growth during zero stress aging.

	Initial Crack Length	Crack Sharpness Amplification Factor	Crack Speed Phase 1	Crack Speed Phase 2
	$a_0$ [μm]	$\vartheta$ -	$\frac{K_0^I(\vartheta - \xi_{sizing})}{\rho_{glass}}$ [μm/s]	$\frac{K_0^{II}(\vartheta - \xi_{sizing})}{\rho_{glass}}$ [μm/s]
<b>Sized Fibers</b>	0.2	993	$7.0 \cdot 10^{-6}$	$1.6 \cdot 10^{-6}$
<b>Desized Fibers</b>	5.9	993	$7.0 \cdot 10^{-6}$	$1.6 \cdot 10^{-6}$

The speed of the advancing crack is very slow. It takes about a minute to progress by the length of a chemical bond. This slow speed is sufficient to reduce the sized fiber’s strength by more than 30% in a month, however. The strength loss is governed by the crack speed divided by the crack length, which means the longer the initial crack length, the less significant is the effect of zero stress aging.

### 5. Discussion

This section concentrates on the results obtained for glass fiber bundles exposed to warm water. The other results of carbon fibers and glass in toluene only confirmed the expected behavior of no change of properties. Nonetheless, it is useful to have this documented.

The zero stress aging in distilled water at 60 °C caused a 33% drop of strength within 90 days of exposure. General drops in strength of glass fibers have been reported before [11,17–22], but not for R-glass. Previous approaches to model the strength degradation were based on semi-empirical formulas, as described by Equation (12). Experimental data in this study, and also the studies reported in the literature, show a fair amount of scatter. This makes it difficult to compare the accuracy of the models. Roughly speaking, however, the results found here agree with the previous studies performed on different types of glass fibers. All show a significant decrease in strength with exposure time.

Linking the strength degradation results to the chemical dissolution of glass gives a possible quantitative link to the concept that the crack growth must somehow be related to a corrosion process. The fact that the experimental data can be well modeled by the dissolution constants  $K_0^I$  and  $K_0^{II}$ , representing the two dissolution phases, shows that crack growth also is influenced by the two phases of dissolution observed for fiber bundles [16] and also other types of glass [15]. We attempted to fit the experimental data with only one of the  $K_0$  factors, but this did not work. The fact that the two dissolution phases need to be considered also may explain why previous authors could not agree on the shape of the strength loss curve. Different betas were tried in Equation (12) to fit the data, while a two-step process as described here in Equations (14a) and (14b) should be used.

It was good that exactly the same model parameters also could explain the behavior of the desized fibers. However, the desizing lowered the initial strength of the fibers by a factor five, which makes the fibers of no practical use and somewhat non-representative. Whether the model suggested here stands up to other more realistic cases remains to be seen and should be tested.

The crack sharpness amplification factor  $\vartheta$  has a physical meaning in this model, but it enters the model as the fraction  $\frac{\vartheta}{a_0}$  in Equations (14a) and (14b) (the small  $\xi_{sizing}$  can be ignored). The initial crack length  $a_0$  is not a well-defined property, since the surface energy  $\gamma$  is not well known. This means  $\vartheta$  also compensates for uncertainties in  $a_0$ . It can be seen from this study that the magnitudes of the parameters in the model make physical sense, but to determine the values properly, more tests would be needed.

The authors measured a wide set of dissolution constants on glass fiber bundles in water at different temperatures and pH values [15]. The constants for phase 1 and 2 are listed in Table 4.

**Table 4.** Glass dissolution rate constants obtained for Phase I and II for the total glass dissolution at different temperatures and pH [15].

T [°C]	60	60	60	60	25	40	80
pH	5.8	10	7	4	5.8	5.8	5.8
$K_0^I$ [g/m <sup>2</sup> ·s]	$1.82 \cdot 10^{-8}$	$1.39 \cdot 10^{-7}$	$5.46 \cdot 10^{-8}$	$8.48 \cdot 10^{-8}$	$1.04 \cdot 10^{-8}$	$1.37 \cdot 10^{-8}$	$4.24 \cdot 10^{-8}$
$K_0^{II}$ [g/m <sup>2</sup> ·s]	$4.05 \cdot 10^{-9}$	$1.11 \cdot 10^{-7}$	$4.85 \cdot 10^{-8}$	$6.24 \cdot 10^{-8}$	$1.42 \cdot 10^{-9}$	$2.72 \cdot 10^{-9}$	$1.47 \cdot 10^{-8}$

Inserting the dissolution constants into Equations (14a) and (14b) gives the strength change of the fiber bundles due to zero stress exposure. The predictions are shown in Figure 5, together with the experimental results that were taken at 60 °C and a neutral pH (at 60 °C) of 5.8. The combination of high temperature (60 °C) and not neutral pH is predicted to give rather rapid degradation in strength. Increasing the temperature to 80 °C also increases the strength loss, but less than the pH change. Lowering the temperature decreases strength loss but, even at room temperature, a noticeable strength degradation is predicted.

Some fiber strength testing under these conditions should be done to confirm the validity of the predictions. We plan to do this in the future. Since the dissolution tests can be done fairly easily, they could be more convenient for predicting strength reductions than fiber bundle testing. More importantly, the dissolution constants are directly related to chemical reactions and Arrhenius extrapolations, allowing the prediction of properties at a wide set of conditions.

This paper investigated R-glass, which is becoming popular for structural applications [15,16,35]. The model should be applicable to other types of glass as well, as SiO<sub>2</sub> is the major component in virtually all types of glass [15] and SiO<sub>2</sub> dominates the dissolution process, at least in phase 2.

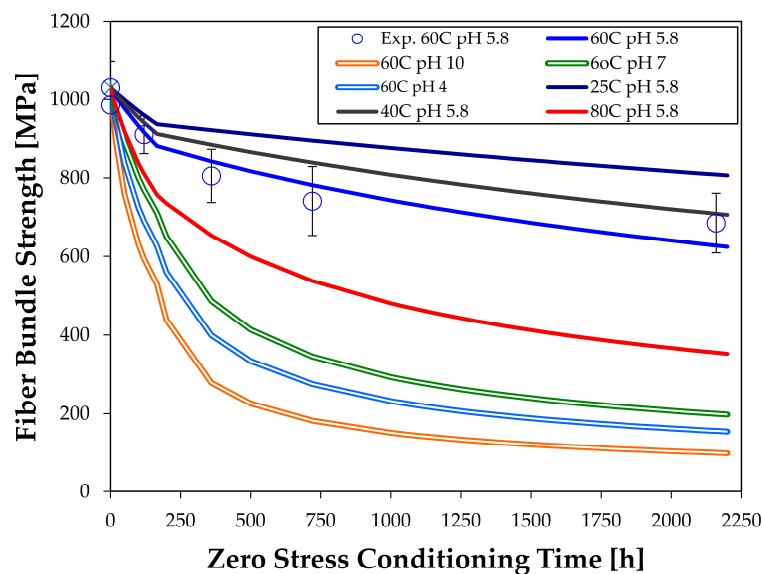


**Figure 5.** Theoretically, sized glass fiber bundle strength changes due to zero stress aging in water at different temperatures and pH. Experimental results were measured for 60 °C at pH 5.8.

It was mentioned in the introduction that this investigation is a step for modelling the strength loss of composites (fiber reinforced plastics, FRP). Considering a composite, the fibers are protected by the matrix and water access is limited, even if the matrix is saturated with water. Removing the ions from the glass and bringing them outside of the composite will be slower. This means the dissolution constants used here are too high for the embedded fibers. Regarding most cases, the fibers also will be stressed when exposed to water. This effect would increase the crack speed as the pressure term in Equation (4) would get activated. The approach shown here helps to explain the mechanisms involved in the fiber degradation.

## 6. Conclusions

A model was developed that can quantitatively link the strength reduction of glass fiber bundles in water at zero stress to the chemical dissolution kinetics of glass ions migrating into the surrounding water.

The model is based on basic concepts: the Griffith model for strength, a crack sharpness amplification factor linked to thermodynamics of surfaces and a zero-order dissolution model for glass.

The dissolution of glass happens in two phases, during an initial disorderly phase and a subsequent steady state phase. The strength reduction model reflects this behavior and makes it different from all previously developed empirical models.

The agreement of the model with experimental results is reasonable but more testing should be done to obtain the model parameters more accurately, over longer times and to confirm the model's validity. Tests were done for R-glass, but it is expected that the principal approach should be valid for any glass.

The model allows predictions of temperature and pH dependence on strength loss, as long as dissolution constants can be found. Since the dissolution constants are linked to standard Arrhenius type dependencies, interpolation of measured values can be easily done.

Experimentally, glass fibers in toluene and carbon fibers in water or toluene did not show any strength changes within the experimental error. Since no chemical reaction happened between the fibers and the liquids in these cases, this result was expected, but it is useful to have it confirmed.

The understanding of the mechanisms of fiber degradation developed here should be useful for characterizing the strength degradation of fibers embedded in a matrix in composites. However, the results cannot be directly used since the dissolution kinetics will be different in a composite, probably slower.

**Author Contributions:** Conceptualization, A.T.E. and A.E.K.; Methodology, A.T.E. and A.E.K.; Software, A.T.E. and A.E.K.; Validation, A.T.E. and A.E.K.; Formal Analysis, A.T.E., A.E.K., A.I.G. and E.S.; Investigation, A.E.K.; Resources, A.T.E. and A.E.K.; Data Curation, A.T.E. and A.E.K.; Test Set-Up and Testing; A.E.K. and E.S.; Writing—Original Draft Preparation, A.T.E., A.E.K. and A.I.G.; Writing—Review and Editing, A.T.E., A.E.K. and A.I.G.; Visualization, A.T.E., A.E.K. and A.I.G.; Supervision, A.T.E. and A.E.K.; Project Administration, A.T.E.; Funding Acquisition, A.T.E.

**Funding:** This research was funded by The Research Council of Norway (Project 245606/E30 in the Petromaks 2 programme).

**Acknowledgments:** This work is part of the DNV GL led Joint Industry Project “Affordable Composites” with nineteen industrial partners and the Norwegian University of Science and Technology (NTNU). The authors would like to express their thanks for the financial support from The Research Council of Norway (Project 245606/E30 in the Petromaks 2 programme). The authors are thankful to Erik Sæter for designing the tensile grips and helping to start the experiments and Erwan Leneveu and Apolline Mayeur for some help with the tests. Andrey is especially grateful to Oksana V. Golubova.

**Conflicts of Interest:** The authors declare no conflict of interest.

## Appendix A

**Table A1.** Complete set of experimentally obtained tensile bundle strength of aged glass and carbon fiber bundles.

Aging Time [h]	Sized GF Strength in Water [MPa]	Desized GF Strength in Water [MPa]	Sized GF Strength in Toluene [MPa]	CF Strength in Water [MPa]	CF Strength in Toluene [MPa]
0 (unaged)	1023, 901, 1001, 1101, 1098, 1054, 1033	185	1023, 901, 1001, 1101, 1098, 1054, 1033	2132, 2171, 1923, 2117	2132, 2171, 1923, 2117
0.17 (10 min)	994, 984, 988, 970, 994	139	987, 1026, 1129, 974	2270, 2553, 2404, 2232, 2277	2203, 1994, 2273, 2445, 2184
24 (1 day)	-	146	-	-	-
72 (3 days)	-	177	-	-	-
120 (5 days)	942, 920, 922, 817, 882, 907, 997, 902, 898	145	1035, 845, 916, 929, 938	2279, 2124, 2349, 2347	2139, 2203, 1966
192 (8 days)	-	176	-	-	-
240 (10 days)	-	211	-	-	-
360 (15 days)	700, 805, 823, 809, 890	143	934, 906, 940, 924, 938	2327, 2287, 2450, 2337, 2076, 2294	2166, 2203, 2380, 2121
528 (22 days)	-	205	-	-	-
720 (30 days)	810, 721, 620, 711, 841	220	1039, 915, 958, 913, 954	2300, 2339, 2350, 2262, 2355	2188, 2332, 2248, 2374
2160 (90 days)	702, 621, 730, 779, 595	-	1014, 1042, 948, 901, 846	2227, 2328, 2270, 2518, 2310	-

## References

1. ISO 527. *Plastics—Determination of Tensile Properties*; International Organization for Standardization: Geneva, Switzerland, 2019.
2. ASTM. *D3039 Standard Test Method for Tensile Properties of Polymer Matrix Composite Materials*; ASTM International: West Conshohocken, PA, USA, 2017. [[CrossRef](#)]
3. Lasn, K.; Klauson, A.; Echtermeyer, A.T. Back-calculation of ply elastic moduli for cross-ply laminates. *Mech. Compos. Mater.* **2014**, *51*, 55–68. [[CrossRef](#)]
4. MIL-HDBK-17-1F. *Polymer Matrix Composites, Volume 1: Guidelines for Characterization of Structural Materials*; U.S. Department of Defense: Washington, DC, USA, 2002.
5. Hart-Smith, L.J. Backing Out Equivalent Unidirectional Lamina Strengths from Tests on Cross-Ply Laminates. In Proceedings of the 37th International SAMPE Symposium, Anaheim, CA, USA, 9–12 March 1992; pp. 977–990.
6. Griffith, A.A. The Phenomena of Rupture and Flow in Solids. *Philos. Trans. R. Soc. A: Math. Phys. Eng. Sci.* **1921**, *221*, 163–198. [[CrossRef](#)]
7. Horstman, R.; Peters, K.; Enright, C.; Meltzer, R.; Vieth, M.B.; Bush, A. Stress Intensity Factors for Single-Edge-Crack Solid and Hollow Round Bars Loaded in Tension. *J. Test. Eval.* **1981**, *9*, 216–223. [[CrossRef](#)]
8. Inglis, C.E. Stresses in a plate due to the presence of cracks and sharp corners. *Proc. Inst. Naval. Archit.* **1913**, *60*, 219–241.
9. Orowan, E. Energy Criteria of Fracture. *Weld. J.* **1955**, *34*, 157–160.
10. Charles, R.J. Static Fatigue of Glass. I. *J. Appl. Phys.* **1958**, *29*, 1549–1553. [[CrossRef](#)]
11. Charles, R.J. Static Fatigue of Glass. II. *J. Appl. Phys.* **1958**, *29*, 1554–1560. [[CrossRef](#)]
12. Wiederhorn, S.M.; Bolz, L.H. Stress Corrosion and Static Fatigue of Glass. *J. Am. Ceram. Soc.* **1970**, *53*, 543–548. [[CrossRef](#)]
13. Freiman, S.W.; Wiederhorn, S.M.; Mecholsky, J.J.J. Environmentally Enhanced Fracture of Glass: A Historical Perspective. *J. Am. Ceram. Soc.* **2009**, *92*, 1371–1382. [[CrossRef](#)]
14. Krauklis, A.E.; Echtermeyer, A.T. Dissolving Cylinder Zero-Order Kinetic Model for Predicting Hygrothermal Aging of Glass Fiber Bundles and Fiber-Reinforced Composites. In Proceedings of the 4th International Glass Fiber Symposium, Aachen, Germany, 29–30 October 2018; Gries, T., Pico, D., Lüking, A., Becker, T., Eds.; Verlag Mainz: Aachen, Germany, 2018; pp. 66–72, ISBN 978-3-95886-249-4.
15. Krauklis, A.; Gagani, A.I.; Vegere, K.; Kalnina, I.; Klavins, M.; Echtermeyer, A.T. Dissolution Kinetics of R-Glass Fibres: Influence of Water Acidity, Temperature, and Stress Corrosion. *Fibers* **2019**, *7*, 22. [[CrossRef](#)]
16. Krauklis, A.; Echtermeyer, A.T. Long-Term Dissolution of Glass Fibers in Water Described by Dissolving Cylinder Zero-Order Kinetic Model: Mass Loss and Radius Reduction. *Open Chem.* **2018**, *16*, 1189–1199. [[CrossRef](#)]
17. Schultheisz, C.; McDonough, W.; Kondagunta, S.; Schutte, C.; Macturk, K.; McAuliffe, M.; Hunston, D. Effect of Moisture on E-Glass/Epoxy Interfacial and Fiber Strengths. In *Composite Materials: Testing and Design*, 13th ed.; Hooper, S., Ed.; ASTM International: West Conshohocken, PA, USA, 1997; pp. 257–286. [[CrossRef](#)]
18. Armstrong, J.L.; Matthewson, M.J.; Juarez, M.G.; Chou, C.Y. Effect of diffusion rates in optical fiber polymer coatings on aging. In Proceedings of the Optical Fiber Reliability and Testing, Boston, MA, USA, 19–20 September 1999; Volume 3848. [[CrossRef](#)]
19. Kennedy, M.T.; Cuellar, E.; Roberts, D.R. Stress-free aging of optical fibers in liquid water and humid environments: Part 1. In Proceedings of the Fiber Optic Components and Reliability, Boston, MA, USA, 3–6 September 1991; Volume 1580. [[CrossRef](#)]
20. Hasløv, P.; Jensen, K.B.; Skovgaard, N.H. Degradation of Stressed Optical Fibers in Water: New Worst-case Lifetime Estimation Model. *J. Am. Ceram. Soc.* **1994**, *77*, 1531–1536. [[CrossRef](#)]
21. Barbero, E.J.; Damiani, T.M. Phenomenological Prediction of Tensile Strength of E-Glass Composites from Available Aging and Stress Corrosion Data. *J. Reinf. Plast. Compos.* **2003**, *22*, 373–394. [[CrossRef](#)]
22. Lara-Curzio, E. Oxidation Induced Stress-Rupture of Fiber Bundles. *J. Eng. Mater. Technol.* **1998**, *120*, 105–109. [[CrossRef](#)]
23. *3B Fibreglass Technical Data Sheet*; HiPer-tex W2020 Rovings; 3B: Herve, Belgium, 2012.
24. Weibull, W. A Statistical Distribution Function of Wide Applicability. *J. Appl. Mech.* **1951**, *18*, 293–297.

25. R'Mili, M.; Moevus, M.; Godin, N. Statistical fracture of E-glass fibres using a bundle tensile test and acoustic emission monitoring. *Compos. Sci. Technol.* **2009**, *68*, 1800–1808. [[CrossRef](#)]
26. Chi, Z.; Chou, T.-W.; Shen, G. Determination of single fibre strength distribution from fibre bundle testings. *J. Mater. Sci.* **1984**, *19*, 3319–3324. [[CrossRef](#)]
27. McCartney, L.N.; Smith, R.L. Statistical Theory of the Strength of Fiber Bundles. *J. Appl. Mech.* **1983**, *50*, 601–608. [[CrossRef](#)]
28. Platt, M.M.; Klein, W.G.; Hamburger, W.J. Mechanics of Elastic Performance of Textile Materials: Part IX: Factors Affecting the Translation of Certain Mechanical Properties of Cordage Fibers into Cordage Yarn. *Text. Res. J.* **1952**, *22*, 641–667. [[CrossRef](#)]
29. Hansen, A.; Hemmer, P.C.; Pradhan, S. *The Fiber Bundle Model: Modeling Failure in Materials*; Wiley-WCH: Weinheim, Germany, 2015; ISBN 978-3-527-67198-4.
30. Torayca. T700S datasheet. In *Technical Datasheet No. CFA-005*; Torayca Carbon Fibers Inc.: Santa Ana, CA, USA, 2013.
31. Wiederhorn, S.M. Fracture Surface Energy of Glass. In Proceedings of the 70th Annual Meeting, The American Ceramic Society, Chicago, IL, USA, 24 April 1968.
32. Shand, E.B. Correlation of Strength of Glass with Fracture Flaws of Measured Size. In Proceedings of the Fall Meeting of the Glass Division, The American Ceramic Society, Bedford Springs, PA, USA, 14 October 1960.
33. Lawn, B.R. *Fracture of Brittle Solids, 2nd ed*; Cambridge University Press: Cambridge, UK, 1993.
34. Champomier, F.P. Crack Propagation Measurements on Glass: A Comparison Between Double Torsion and Double Cantilever Beam Specimens. In *Fracture Mechanics Applied to Brittle Materials*; ASTM STP 678; Freiman, S.W., Ed.; American Society for Testing and Materials: West Conshohocken, PA, USA, 1979; pp. 60–72.
35. Krauklis, A.E. Environmental Aging of Constituent Materials in Fiber-Reinforced Polymer Composites. Ph.D. Thesis, NTNU, Trondheim, Norway, 2019.



© 2019 by the authors. Licensee MDPI, Basel, Switzerland. This article is an open access article distributed under the terms and conditions of the Creative Commons Attribution (CC BY) license (<http://creativecommons.org/licenses/by/4.0/>).